

Resource Allocation in Networked Joint Radar and Communications

Sevda Şahin and Tolga Girici

Dept. of Electrical and Electronics Engineering

TOBB University of Economics and Technology

Ankara, Turkey

{sevda.sahin,tgirici}@etu.edu.tr

Abstract—In today’s world, particularly in civilian sectors where situational awareness is paramount, research is being conducted on concepts that enable the joint realization of both sensing and communication functions with the upcoming 6G technology planned for near-future deployment, especially in sectors like automotive. On the other hand, efforts in the military domain to enhance situational awareness and counter evolving air threats have gained momentum with the development of systems incorporating multiple sensors for joint operation, known as radar network architectures. However, when multiple radar systems operate together, bandwidth allocation must be performed in order to avoid interference. As a contribution to the literature, this study proposes a joint radar and communication network concept applied to air defense systems, aiming to enhance their situational awareness by adopting the joint radar and communication concept commonly addressed in civilian applications. Additionally, a resource optimization problem has been addressed to maximize the performance of both radar and communication functions within the joint radar and communication network.

Index Terms—Radar network, resource management, joint radar and communication network, situational awareness, integrated sense and communication (ISAC).

I. INTRODUCTION

Modern air threats possess capabilities/features that limit the detection and engagement capabilities for air defense systems, such as high speed, superior maneuverability, advanced avionics equipment, individual and coordinated electronic warfare capabilities, and low radar cross-section. These technological advancements in air threats necessitate air defense systems to have capabilities such as expanded coverage, joint operations, advanced sensor systems, sensor fusion, protection against electronic warfare techniques, and effective communication with centralized command and control systems of regional air defense systems [1], [2]. As a result, with the evolving capabilities of air threats, the danger zones requiring alarm generation and preventive measures for defended regions have expanded, consequently necessitating an increase in the ranges of air defense systems. This necessitates an increase in the number of radars scanning the defended area for an air defense system, and the planning of a strategy that enables these radars to effectively utilize shared resources. Multiple radar stations strategically distributed over a geographical area and work together to provide comprehensive monitoring and surveillance, over a large region is called a *radar network* [3].

In the literature, there are numerous recent studies on this method referred to as a radar network [4]–[17]. On the other hand, for radar networks to operate effectively together, there is a need for an efficient communication infrastructure such as Link-16 [18], [19]. When a separate communication system is used on the platform, this raises an interoperability issue that needs to be addressed both in terms of physical system deployment and in the frequency spectrum due to the interference between radar and communication systems. This critical interoperability problem, which manifests itself not only in military systems but also in civilian systems, can also be addressed through the concept of joint radar and communication systems (or dual-function radar and communications (DFRC)) [20], which is currently being researched in civilian applications.

In particular, in the automotive sector, research is being conducted on joint radar and communication systems to enable radar and communication systems placed on the same platform to operate together without interfering with each other’s functions, with the aim of increasing situational awareness. As a solution for this problem, the integration of radar and communication system hardware, along with the use of a joint waveform for both functions, not only addresses interference issues between systems but also enhances joint mission effectiveness. In this context, there are numerous studies in the literature focused on creating joint waveform [21]–[25]. These studies are primarily divided into two main areas: communication over radar signals and sensing over communication signals. In both scenarios, the waveform transmitted varies randomly according to the communication signal it carries. While this randomness is expected for a communication system, it adversely affects radar system performance because the radar system operates under the assumption that the reflected signal from the target region remains unchanged during the pulse integration time.

In our previous work, a new radar receiver was proposed by us to mitigate this negative impact [26]. In this study, we worked on the concept of using the integrated sensing and communications (ISAC) to enhance the situational awareness of air defense systems, assuming that the negative effects of communication symbols on the radar receiver were eliminated using the matched filter bank proposed earlier by us. As a contribution to the literature, we worked on optimizing resource sharing to maximize both communication and radar

functions in a radar network consisting of N radars, each with a mono-static operational concept, using a joint waveform with linear frequency modulation (LFM) based on the ISAC system concept in Fig. 1. This study assumes that all joint radar and communication systems in the network collect data, which is then processed by a single Command and Control Center (CCC) responsible for resource allocation. In the default scenario, these systems use a single waveform to detect targets and transmit data regarding the detected targets and their own system statuses to the central command and control system. This central command and control system can also perform the task of allocating the resources such as energy, bandwidth, beams as well as assigning targets to individual radars. This resource allocation problem in radar networks has been a popular research topic in the recent years. First time in the literature, we address the resource allocation problem in radar networks that perform joint radar and communications.

A. Related Work

Utilizing networks for sensing has been a popular research topic in recent years. In [4] the authors studied a networked localization problem and proposed an algorithm to optimize the transmit powers for wireless and radar network localization of a single target. In [5] and [6] a clustered network of multiple radars was considered and a game-theoretic scheme was proposed to achieve a target detection performance. In this scheme, there is coordination among members of a cluster but no inter-cluster coordination. The authors in [7] optimize the dwell times in a radar sensor network for tracking purposes. Another area of research on networked radar, is task allocation and scheduling [8]. Authors in [9], [10] consider the problem of assignment of radars to targets jointly with power allocation. A two step semidefinite programming solution and a two step convex programming solution for this nonconvex optimization problem was proposed in [9] and [10], respectively. In [11] target assignment, dwell and bandwidth for multi-target, multi-radar tracking. The resulting nonlinear mixed-integer optimization problem is solved in three stages. For multi-radar, multi-beam MIMO radar network the papers [12], [13] jointly optimize the beam assignment and power allocation in order to maximize the tracking accuracy. An iterative algorithm is proposed in order to find a solution to this mixed integer nonlinear problem. The paper [13] additionally considers detection threshold as an optimization parameter. The authors in [14] tackles a similar problem in order to minimize a weighted sum of probability of intercept and target tracking performance. The paper [15] solves a joint target assignment, power and bandwidth allocation problem for a similar scenario. Physical resources, such as antenna aperture (i.e. physical antenna elements) is added to the problem as an optimization parameter in [16]. In [17] and [27] the authors consider a multi-radar network and optimize the bandwidth allocation to the individual radars in order to satisfy a radar SNR constraint. These authors also considered communication links. However, communication and radar functions are assumed to exist in different time intervals.

The work in [28] is a survey study on resource allocation in joint radar and communications. However the stud-

ies mentioned in this survey almost exclusively assume a single radar/communications transceiver and allocate time, bandwidth, subchannels, power or antennas between radar and communication functions in a joint radar and communications transceiver. They don't assume multiple radars and allocate resources among them. One exception can be [29], where carrier sense multiple access (CSMA) scheme is proposed for the multiple access of automotive radars in the vehicles. However, the system model is very different than our scenario. They assume that radar and communications signals are sent in different time intervals, which is not spectrally efficient. Besides, random access results in collisions and can be detrimental in air defense scenarios.

B. Contributions

To the best of our knowledge, this is the first work that addresses resource allocation in a radar network that performs dual function radar and communications. We assume that the radar nodes transmit LoRa-like signals [30] that are used for both radar target tracking and for communications with a Command and Control Center (CCC). We formulate and solve an integer programming problem in order jointly optimize the subchannels allocated to each radar and spreading factor in order to jointly control radar and communications performance.

II. SYSTEM MODEL

We consider N monostatic radar transceivers that are randomly positioned on an area. Each of these transceivers transmit a pulse burst, where τ_n is the pulse duration of radar transceiver n . Let T_n be the pulse repetition interval (PRI) of transceiver n . In this work we assume that $T_n = T, \forall n$. Let r_n and v_n be the distance (range) from transceiver to its target and target's velocity, respectively. In this work we assume that each transceiver has its own (assigned) target ¹.

There is a total bandwidth of W , which is shared among the radar transceivers. This resource allocation and coordination is performed by the CCC. The total bandwidth is divided into $K = W/B$ subchannels, where $K > N$ and B is the subchannel bandwidth, as shown in the lower part of Fig. 1. Each transceiver is allocated an adjacent group of subchannels. A disjoint set of subchannels is allocated for each transceiver, so that there is no interference among radar transceivers. For example in Fig. 1, radar 1, 2, 3, 4 and 5 are allocated, 2, 3, 4, 3 and 8 subchannels, respectively. For a total of K subchannels, if a radar transceiver is to be allocated a adjacent subchannels, this can be done in $K - (a - 1)$ ways ². Therefore the number of available allocation patterns becomes at most $C = \sum_{a=1}^K K - (a - 1) = \frac{K^2}{2} + \frac{K}{2}$ [31]. Let \mathcal{C} be the set of allocation patterns. The number of subchannels allocated to a radar transceiver may be limited, which reduces C . Center frequency and bandwidth of allocation pattern c are denoted by f_c and W_c , respectively.

¹Target assignment optimization is a possible subject to future work.

²For example for $K = 5$ subchannels and $a = 2$ subchannel allocations, a radar can be allocated the sets $\{1, 2\}$, $\{2, 3\}$, $\{3, 4\}$ and $\{4, 5\}$, hence there are $5 - (2 - 1) = 4$ alternative ways.

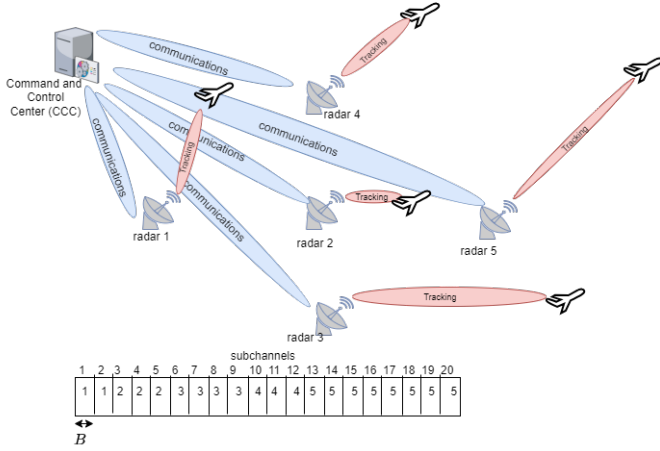


Fig. 1: Operational concept illustration of joint communication and target sensing system. In the figure, there are $N = 5$ radars and $K = 20$ subchannels. As seen in the lower part of the figure, different number of subchannels can be allocated to different radars in order to jointly optimize radar and communications performance.

A. ISAC System Waveform Design

In this study, we used chirp radar waveform to implement both radar and communication functions as defined in [23]. Unlike the study in [23], we performed the analyses for pulse modulated radar with chirp in each pulse.

A chirp radar signal with pulse width τ , bandwidth W and initial phase ϕ_0 is expressed by (1) [23].

$$S_{chirp}(t) = e^{j(\pi\mu t^2 + 2\pi f_c t + \phi_0)} \quad (1)$$

Here f_c is the carrier frequency and μ is the chirp rate. Also, t is an element of the set $[-\tau/2, \tau/2]$. The chirp rate μ is given in (2).

$$\mu = \frac{W}{\tau} \quad (2)$$

In order to send the communication symbols within the radar pulse, different initial frequencies are used for the chirp signal for each symbol. In the offered ISAC system waveform, each pulse is divided into two and a chirp with a different initial frequency is used for each segment. The mathematical expression of this signal is given in (3).

$$S_{RadCom}(t) = S_{chirp}(t - \Delta t_m) \quad (3)$$

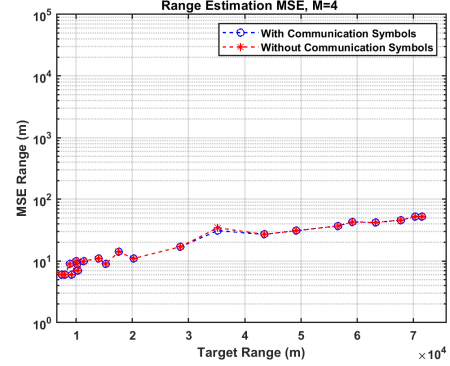
Δt_m is determined by (4).

$$\Delta t_m = \frac{m\tau}{M}, m \in \{1, 2, \dots, M-1\} \quad (4)$$

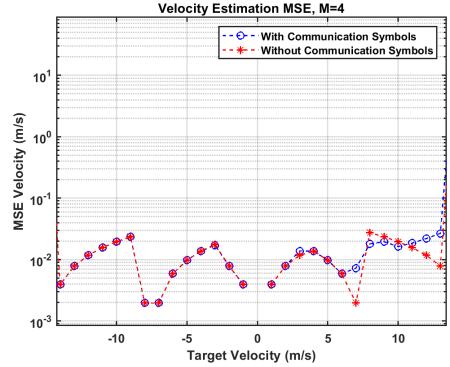
Here, M is the number of symbols. In the LoRa technology, $M = 2^{SF}$, where SF is known as the spreading factor. In this work we use LoRa-like signals in joint radar and communications. With this technique, $\log_2 M = SF$ bits can be transmitted per pulse burst.

In ISAC application, since the waveform changes randomly according to the transmitted communication symbol during the integration process, this affects both the range and velocity estimation negatively. In the method we proposed in [26],

aligned with the mono-static pulse radar operational concept, each received pulse at the radar receiver undergoes processing by passing through a matched filter selected from the filter bank in order to minimize the effect of randomness of communication symbols on radar detection performance. These matched filters are compatible with the communication symbol sent by the transmitter. The range and velocity estimation performance of this technique are compared with conventional radar in Fig. 2.



(a) Range MSE



(b) Velocity MSE

Fig. 2: Range and velocity estimation performance without communication symbols and with communication symbols for matched filter bank radar receiver, $M = 4$. (a) Range error, (b) Velocity error

As seen from these simulation results, effects of communication symbol on the radar performance is negligible.

B. Radar Performance

Received SNR at the radar receiver n is as follows,

$$\gamma_{n,c}^r = \frac{P_t c^2 G_n^2 \sigma_n}{(4\pi)^3 f_c^2 r_n^4 N_o W_c} \quad (5)$$

where $c = 3 \times 10^8$ m/s is the speed of light, P_t is the transmit power, G_n is the antenna gain and σ_n is the radar cross section of target n . We neglected atmospheric losses. $N_o W_c$ is the noise power.

We assume that there is a command and control center (CCC) in the area that performs resource allocation for the transceivers. For this purpose, radar transceivers regularly

inform the CCC about the range, velocity and SNR information. Same transceivers are utilized for both radar and communications purposes. In order to support simultaneous radar and communication transmissions, the radar transceivers use the mainlobe of the antenna for radar and a sidelobe of the antenna for communications [32], [33]. In [32] the sidelobe is turned on and off (with minimal distortion in the mainlobe) in order to convey information. In our case, a **phased array antenna configuration is considered, where the mainlobe is dedicated to target tracking, and communication with the command and control center occurs through a sidelobe.** Given that the target is located at a greater distance than the CCC, the electronically steered beam tracks the target at a relatively slow rate. Consequently, it is assumed that the communication link with the command center remains stable and unaffected by the beam's target tracking dynamics. As a result the same ISAC signal can be transmitted both from the mainlobe and sidelobe. Therefore it is not mandatory to apply separate beamforming optimization for the sidelobe. We assume that the targets are in the air and CCC is on the ground and there is a stable communication channel between the radar and the CCC.

We assume that the radar transceivers use Linear Frequency Modulated (LFM) pulse signals with suitable parameters [30]. For example, allocating k_n adjacent subchannels to radar n makes the transceiver bandwidth equal to $W_{n,c} = k_n B$ Hz. Spreading factor of transceiver n is denoted by SF_n and it is selected from the set $S\mathcal{F}$. Pulse duration is directly related to the spreading factor as $\tau_{n,c} = \frac{2^{SF_n}}{W_{n,c}}$. At each *round*, N_p pulses are sent, with a pulse repetition interval of T_n , then a target parameter estimation is made by the radar transceiver. Each pulse can be used to encode SF_n bits. Each pulse in a round can be different, since they are also used to encode information bits. Hence, the total number of bits sent in a round is $SF_n N_p$. Radar transceivers transmit N_p pulses and combine them for range and Doppler processing. Then, they transmit the range, velocity, SINR and other necessary information to the center.

We measure radar performance with the Delay and Doppler estimation error. From the literature, Cramer-Rao lower bound (CRLB) for the maximum likelihood time delay estimator is [34]–[36],

$$\begin{aligned} \sigma_{t_{0,c},SF_s}^2 &\geq \frac{3}{2\pi^2 W_c^2 \gamma_{n,c}^r 2^{SF_s} N_p} \left[1 + \frac{1}{N_p^2 - 1} \left(\frac{\tau_{n,c}}{T} \right)^2 \right] \\ &= \frac{3}{2\pi^2 W_c^2 \gamma_{n,c}^r 2^{SF_s} N_p} \left[1 + \frac{1}{N_p^2 - 1} \left(\frac{2^{SF_s}}{T W_{n,c}} \right)^2 \right] \\ \sigma_{t_{0,c},SF_s}^2 &\simeq \frac{3/2}{\pi^2 W_c^2 \gamma_{n,c}^r 2^{SF_s} N_p} \end{aligned} \quad (6)$$

The last approximation is quite accurate if the number of pulses is large. This expression depicts that as the spreading factor and number of pulses increase, the time delay (and range) accuracy improves.

Again from the literature, CRLB for the Doppler estimation is [34], [37],

$$\sigma_{f_{d,c},SF_s}^2 \geq \frac{f_c^2}{c^2} \frac{6}{16\pi^2 \tau_n N_p^2 (N_p - 1) \gamma_{n,c}^r W_c T^2} \quad (7)$$

$$= \frac{f_c^2}{c^2} \frac{3}{8\pi^2 2^{SF_s} N_p (N_p^2 - 1) \gamma_{n,c}^r T^2} \quad (8)$$

using $\tau_n = 2^{SF_s}/W_c$. As seen from the formula, Doppler frequency estimation accuracy improves with increasing PRI, Spreading factor and SNR. Moreover, it dramatically improves with number of pulses.

C. Communication Performance

Let d_n be the distance of transceiver n from the CCC. The received SNR at the *communication receiver* (i.e. CCC) signal becomes,

$$\gamma_{n,c}^c = \frac{P_t c^2 G_n^s G^c}{(4\pi)^2 f_c^2 d_n^2 N_o F W_c} \quad (9)$$

where G_n^s is the sidelobe gain of the radar transceiver. G^c and F are the receive antenna gain and noise factor of the CCC receiver. Again note that sidelobe gain G_n^s is much lower than the mainlobe gain G_n so that communication signal does not mislead the radar tracking process. Note that Eq. (5) involves the 4th power of the target distance and the mainlobe gain, while Eq. (9) involves the 2nd power of the communications (radar-CCC) distance and the sidelobe gain.

We assume a Rayleigh fading communication channel. We also assume that ISAC transceivers and CCC are located on an open area. According to [38] in open areas delay spread is between 0.1 to 1 microseconds. Coherence bandwidth is roughly the inverse of delay spread, which corresponds to 1 – 10 MHz coherence bandwidth. Therefore it is reasonable to assume that a 1 MHz subchannel experiences a flat fading. For a Rayleigh fading channel, the authors in [39] obtained an approximate closed form formula for the bit error rate (BER) of chirp spread spectrum modulation, which is shown in Eq. (10),

We measure the communication performance as the achievable rate. Achievable rate is $\frac{SF_s}{T}$ bits per second. However, this rate is achieved if the bit error rate in (10) is less than a target P_0^b , which is the maximum bit error rate requirement. Otherwise, the achievable rate is assumed as zero,

$$R_{n,c,s} = \begin{cases} \frac{SF_s}{T} & P_{n,c,s}^b < P_0^b \\ 0 & P_{n,c,s}^b > P_0^b \end{cases} \quad (11)$$

D. Combined Cost Function

In order to take into account timing, Doppler estimation accuracy, along with energy expenditure and data rate, let us define the multiobjective cost $L_{n,c,s}$ as follows

$$\begin{aligned} L_{n,c,s} = \alpha_1 e^{\frac{\sigma_{t_{0,c},SF_s} - \sigma_t^0}{\sigma_t^0}} + \alpha_2 e^{\frac{\sigma_{f_{d,c},SF_s} - \sigma_{f_d}^0}{\sigma_{f_d}^0}} \\ + \alpha_3 \left(0.96 + 86.2 e^{\frac{-7.79 R_{n,c,s}}{R^0}} \right) \end{aligned} \quad (12)$$

This cost parameter combines the delay and Doppler estimation performance, and data rate. Combined cost $L_{n,c,s}$

$$P_{n,c,s}^b \approx \frac{1}{2} \left[Q\left(-\sqrt{2H_{2SF_s-1}}\right) - \sqrt{\frac{2SF_s\gamma_{n,c}^c}{2SF_s\gamma_{n,c}^c+1}} e^{-\frac{2H_{2SF_s-1}}{2(2SF_s\gamma_{n,c}^c+1)}} Q\left(\sqrt{\frac{2SF_s\gamma_{n,c}^c}{2SF_s\gamma_{n,c}^c+1}} \left[-\sqrt{2H_{2SF_s-1}} + \frac{\sqrt{2H_{2SF_s-1}}}{2SF_s\gamma_{n,c}^c+1}\right]\right) \right] \quad (10)$$

is the weighted combination of each component, where α_1 , α_2 and α_3 are the corresponding weights. Parameters σ_t^0 and $\sigma_{f_d}^0$ are the target values for the radar performance, while R^0 is the target data rate. As seen in (12) we chose exponential penalty functions. For example, the first term, $e^{(\sigma_{t_0,c,SF_s}-\sigma_t^0)/\sigma_t^0}$ takes values e , e^2 as the square root delay error doubles and triples the target, respectively. The same holds for the second term, $e^{(\sigma_{f_d,c,SF_s}-\sigma_{f_d}^0)/\sigma_{f_d}^0}$. Finally the third term $0.96+86.2e^{-\frac{7.79R_{n,c,s}}{R^0}}$, found by curve fitting, takes values e , e^2 when the data rate is half and one-third of the target rate, respectively. This is sort of a normalization that is done in order to bring each cost component to the same level. In numerical evaluations we consider only binary weights (i.e. either 1 or 0).

We also assume that the radars have a maximum duty cycle requirement η , where η is between 0 and $\frac{1}{2}$. Additionally, the target shouldn't be in the blind range. Some bandwidth-spreading factor pairs don't satisfy these requirements, therefore they are infeasible.

Finally we assume an energy expenditure constraint. Each radar transceiver uses a fixed power P_t , therefore the amount of energy spent in a pulse becomes

$$E_{n,c} = P_t \tau_{n,c} = P_t \frac{2SF_n}{W_{n,c}} \quad (13)$$

and energy per bit becomes $Eb_{n,c,s} = P_t \frac{2SF_n}{SF_s W_{n,c}}$. Here SF_n is the chosen spreading factor (i.e. bits sent) for ISAC transceiver n , in a PRI, where $SF_n \in \{1, 2, \dots, |\mathcal{SF}|\}$. As the spreading factor increases, pulse duration increases. Increasing pulse duration also increases the blind range and power expenditure. We define E^0 as the maximum energy constraint. As the transmit power is fixed, energy constraint can be translated into a duty cycle constraint.

Let $f_{n,c,s}$ be the binary feasibility parameter, which is zero if the bandwidth-spreading factor pair is infeasible. The duty cycle constraint is as follows,

$$f_{n,c,s} = \begin{cases} 1 & \frac{1}{2} \frac{2SF_n}{W_{n,c}} < \min\left(\frac{r_n}{c}, \eta T, \frac{E^0}{2P_T}\right) \\ 0 & \text{else} \end{cases} \quad (14)$$

Next, we will present the optimization problem.

III. PROBLEM FORMULATION

As explained in Section II, the CCC has to allocate an adjacent group of subchannels to each radar transceiver. Secondly, set of subchannels allocated to each transceiver has to be disjoint. For a total number of K subchannels, there is a total of $C = \frac{K(K+1)}{2}$ allocation patterns.

Let's define the binary allocation variable as $x_{n,c,s}$, which takes value 1 if pattern c of subchannels and spreading factor s is assigned to transceiver n and 0, otherwise. The resulting optimization problem is

$$\max_{x_{n,c,s}, \forall n \in \mathcal{N}, c \in \mathcal{C}, s \in \mathcal{S}} \left\{ \sum_{n \in \mathcal{N}} \sum_{c \in \mathcal{C}} \sum_{s \in \mathcal{S}} L_{n,c,s} f_{n,c,s} x_{n,c,s} \right\} \quad (15)$$

s.t.

$$\sum_{c \in \mathcal{C}} \sum_{s \in \mathcal{S}} x_{n,c,s} = 1, \forall n \in \mathcal{N} \quad (16)$$

$$\sum_{n \in \mathcal{N}} \sum_{c \in \mathcal{C}} \sum_{s \in \mathcal{S}} A_{k,c} x_{n,c,s} = 1, \forall k \in \mathcal{K} \quad (17)$$

$$x_{n,c,s} \leq f_{n,c,s}, \forall n, c, s \quad (18)$$

$$x_{n,c,s} \in \{0, 1\}, \forall n, c, s \quad (19)$$

Here, objective (15) aims to maximize the total net utility. Constraint (16) enforces that for each radar only one subchannel pattern and spreading factor is assigned. Constraint (17) enforces that each subchannel is allocated to only one radar transceiver. Here $\mathbf{A} = [A_{k,c}]$ is a $K \times C$ matrix, which is called the subchannel allocation matrix. Below is an example of \mathbf{A} for $K = 4$ subchannels, which corresponds to $C = 10$ allocation patterns,

$$\mathbf{A} = \begin{bmatrix} 1 & 0 & 0 & 0 & 1 & 0 & 0 & 1 & 0 & 1 \\ 0 & 1 & 0 & 0 & 1 & 1 & 0 & 1 & 1 & 1 \\ 0 & 0 & 1 & 0 & 0 & 1 & 1 & 1 & 1 & 1 \\ 0 & 0 & 0 & 1 & 0 & 0 & 1 & 0 & 1 & 1 \end{bmatrix} \quad (20)$$

Each column of this matrix contains an allocatable subchannel pattern. Array element $A_{k,c}$ is 1 if subchannel k is in pattern c , otherwise it is 0. This matrix is used in the problem formulation above, in order to make it easier to formulate and understand.

Constraint (18) enforces that a pattern and a spreading factor pair is assigned to a radar transceiver, only if it is feasible (i.e. does not violate the blind range and duty cycle requirements.). Finally (19) implies that the optimization variable $x_{n,c,s}$ is binary. This is a binary linear optimization problem and can be solved using standard packages like Python-based pulp library.

IV. SIMULATION RESULTS

In this section we will evaluate the performance of the proposed resource allocation algorithm and compare it with the optimal solution. Table I shows the default simulation parameters. We set target ranges of each target randomly between (r_{min}, r_{max}) and distances to the CCC randomly between (d_{min}, d_{max}) . We assume the same PRI (T) for all radar transceivers.

We will also compare the performance with a benchmark called Equal Bandwidth Allocation (EBA). In this method, available subchannels are equally allocated to the radar transmitters, where each radar gets adjacent subchannels. Then each radar decides a spreading factor that satisfies the duty cycle constraint and maximizes its utility.

Simulation Parameters	Default Values
Number of Radar Transceivers , N	5
Min. Target Range , (r_{min})	10km
Max. Target Range , (r_{max})	75km
Min. Communication Distance , (d_{min})	10km
Max Communication Distance , (d_{max})	30km
Transmit Power , P_t	1kW
Transmit Antenna Gain , G_n	30dB
Noise power spectral density , N_o	-174 dBm
Antenna Sidelobe Gain , G_n^s	0dB
CCC Receive Antenna Gain , G^c	0dB
Radar Carrier Frequency, f_0	10 GHz
Total Bandwidth (W)	20MHz
Subchannel Bandwidth (B)	1MHz
Radar Pulse Repetition Interval (T)	800 μ s
Pulse repetitions per round (N_p)	50
Spreading Factor set, SF	{2, 3, ..., 11, 12}
Radar Pulse Width (τ_n)	$< \frac{T}{2} \mu s, \forall n$
Radar False Alarm Probability	10^{-6}
Radar cross section (σ_n)	$1m^2$
Maximum duty cycle	$\eta = 0.5$
Bit error rate requirement	$P_0^b = 10^{-4}$
Doppler performance requirements	$\sigma_f^0 = 10$ Hz
Delay performance requirement	$\sigma_t^0 = 1$ ns
Energy expenditure constraint	$E^0 = 0.5$ Joule

TABLE I: Simulation parameters and their default values

In Table II we compared 7 different combinations of α parameters in terms of delay and Doppler estimation accuracies and data rate. We did these simulations for $r_{max} = 75$ km, $d_{max} = 30$ km. Results reveal that,

- If $\alpha_1 = \alpha_2 = 0$, then the radar performance is significantly worse.
- If $\alpha_3 = 0$, then the rate performance is significantly worse.
- $(\alpha_1, \alpha_2, \alpha_3) = (1, 1, 1)$ provides the best overall performance.
- $(\alpha_1, \alpha_2, \alpha_3)(0, 1, 1)$ and $(1, 0, 1)$ also perform well. They are quite close to $(1, 1, 1)$ in terms of performance.

$\alpha_1, \alpha_2, \alpha_3$	$\overline{\sigma_{t_0}}$ (ns)	$\overline{\sigma_{f_d}}$ (Hz)	\overline{R} (kbps)
(0, 0, 1)	19.8	9.32	11.0
(0, 1, 0)	20.3	8.52	10.3
(0, 1, 1)	19.2	8.52	10.8
(1, 0, 0)	16.5	9.19	10.2
(1, 0, 1)	16.5	9.16	10.7
(1, 1, 0)	16.5	8.97	10.3
(1, 1, 1)	16.5	8.75	10.7

TABLE II: Performance of the optimal (MIP) solution for different weight combinations

Radar # (n)	r_n	d_n	k_n	SF_n
1	37.1	11.8	3	9
2	56.8	13.7	11	12
3	10.0	16.9	1	6
4	29.7	17.9	3	9
5	19.6	20.8	2	8

TABLE III: Optimal resource allocation for an example scenario.

Table III shows the optimal resource allocation for an example scenario. Columns r_n , d_n , k_n and SF_n are the target range, distance to the CCC, resulting number of allocated

subchannels and spreading factor, respectively. Radar 2 has a very high target range, therefore it gets the highest number of subchannels. This also help reduce the pulse duration and allows a higher spreading factor, without violating the duty cycle constraint. Radar 3 has the closest range, therefore it gets only one subchannel. Due to the close range and duty cycle constraint (blind range) a large spreading factor is not allowed. Radar 5 has a relatively small target range, but a large communication range. In order to support this range it gets a higher spreading factor. In order to do this without violating the duty cycle constraint, it gets two subchannels and reduces to pulse duration to half.

A. Suboptimal Algorithms

In this part we will propose two simple algorithms. These algorithms serve as benchmarks. However, greedy bandwidth allocation performs surprisingly close to optimal.

1) *Equal Bandwidth Allocation (EBA)*: This algorithm allocates equal number of subchannels to all radar transceivers. Without loss of generality we assume that K/N is an integer. Due to the adjacency constraint each radar receives K/N subchannels in the order of radar index. Let c_n be the subchannel pattern index allocated to radar n . Then, the optimal spreading factor s_n is chosen according to $s_n = \arg \max_{f_n, c_n, s=1} \{L_{n, c_n, s}\}$.

2) *Greedy Bandwidth Allocation (GBA)*: Due to its integer nature, the optimal solution has prohibitive complexity, as the number of radars and subchannels increase. We will propose an algorithm that allocates subchannels to radars in a greedy manner. After that, the spreading factor for each ISAC transmitter can be determined separately.

Let's define c_k^0 be the first allocation pattern that has k subchannels. For example in (20) $c_2^0 = 5$. Let us define a $K \times N$ utility matrix \mathbf{U} , where $U_{n,k} = \max_{f_n, c_k^0, s=1} \{L_{n, c_k^0, s}\}$. Pseudo code of the GBA method is shown in Algorithm 1. Line 1 computes the utility matrix and Line 2 gives each ISAC transmitter one subchannel, initially. While loop in Lines 3-6 allocates each remaining subchannel to the node that maximizes the incremental utility. For loop in Lines 7-10 starts from the first subchannel and first ISAC transmitter, and allocates an adjacent set of subchannels (pattern with k_n number of subchannels) to each of them. Line 9 also determines the best spreading factor for each transmitter.

Algorithm 1 Greedy Bandwidth Allocation (GBA)

- 1: Compute, $U_{n,k} = \max_{f_n, c_k^0, s=1} \{L_{n, c_k^0, s}\}, \forall n, k$
 - 2: Initialize, $k_n = 1, \forall n = 1, \dots, N$
 - 3: **while** $\sum_{n=1}^N k_n < K$ **do**
 - 4: Find $n^* = \arg \max_n \{U_{n, k_n+1} - U_{n, k_n}\}$
 - 5: Set, $k_{n^*} = k_{n^*} + 1$
 - 6: **end while**
 - 7: **for** $n=1:N$ **do**
 - 8: Find $c^* = \arg \min_{\sum_{k=1}^K A_{k,c}=k_n \text{ and } \sum_k \{A_{k,c} A_{k,c'}\}=0} \{c\}$
 - 9: Find $s^* = \arg \max_{s \in S} L_{n, c^*, s}$ and set $x_{n, c^*, s^*} = 1$
 - 10: **end for**
-

Table IV shows the average net utility corresponding to the three methods. We did these simulations for $r_{max} = 75\text{km}$, $d_{max} = 30\text{km}$. First of all, it is clear that EBA performs significantly worse than the optimal resource allocation. This shows that optimal method, allocates bandwidth wisely so that increasing spreading factor doesn't cause an excessive increase in duty cycle. Now, let's focus on $(\alpha_1, \alpha_2, \alpha_3) = (1, 1, 1), (1, 0, 1)$ and $(0, 1, 1)$. We can see that GBA algorithm performs very close to the optimal. The difference is less than 7%.

$(\alpha_1, \alpha_2, \alpha_3)$	Optimal	EBA	GBA
(0, 0, 1)	48.8	81.6	55.7
(0, 1, 0)	4.99	6.00	5.12
(0, 1, 1)	53.8	87.6	56.6
(1, 0, 0)	13.2	25.6	13.2
(1, 0, 1)	62.2	107.2	66.6
(1, 1, 0)	18.6	31.6	18.9
(1, 1, 1)	67.6	113.2	72.4

TABLE IV: Average utility comparison of optimal and equal bandwidth resource allocation, with respect to weights

Figure 3 shows the average weighted cost performance of GBA as a function of PRI for different weight combinations. It is seen that the cost first decreases abruptly. There are two main reasons of this. First reason is the sharp decrease in the Doppler error (weighted by α_2). Second reason is the increased range of available spreading factors, which improves both the time delay and Doppler estimation performances (weighted by α_1 and α_2). When the PRI is increased more, the cost starts to increase. Because, Doppler accuracy falls below the target value. But, this time the data rate is decreasing, which increases the third component of the cost (weighted by α_3). So, there is an optimal PRI value. Optimal PRI is $900 - 950\mu\text{s}$ for $(\alpha_1, \alpha_2, \alpha_3) = (1, 1, 1)$, $850 - 900\mu\text{s}$ for $(\alpha_1, \alpha_2, \alpha_3) = (1, 0, 1)$, and $1000 - 1100\mu\text{s}$ for $(\alpha_1, \alpha_2, \alpha_3) = (0, 1, 1)$.

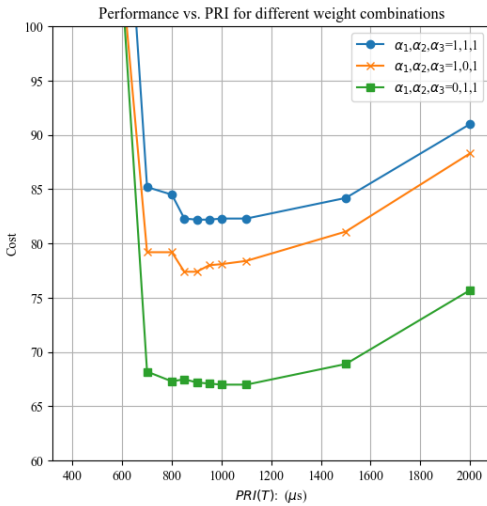


Fig. 3: Performance vs. Pulse Repetition Interval (PRI) for different weight combinations.

Figure 4 shows the radar and communication performance as a function of maximum target range. As maximum target range increases, radar performance (time and Doppler) gets

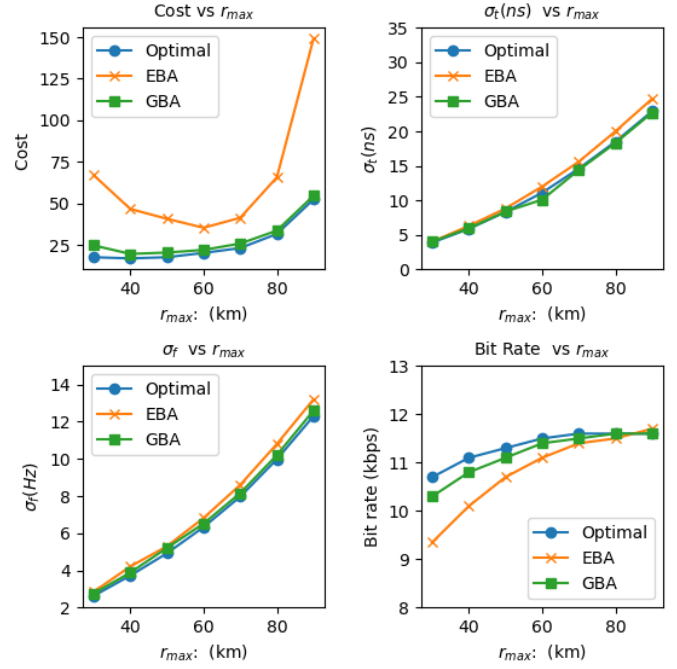


Fig. 4: Performance vs maximum target range (r_{max})

worse, which is expected. As the range increases, maximum allowable duty cycle gets larger according to (14), which increases the data rate. Data rate converges to $\frac{12\text{bits}}{800\mu\text{s}} = 12.5\text{kbps}$. If the range is shorter, the optimal solution and GBA cleverly allocates bandwidth in order to adjust the spreading factor. EBA method has significantly lower utility when compared with the optimal solution and GBA. This shows the importance of optimal bandwidth allocation. Proposed GBA method is very close to the optimal.

Figure 5 shows the radar and communication performance as a function of maximum distance to the CCC (i.e. d_{max}). Target range r_{max} is uniformly distributed between $10 - 75\text{km}$ and maximum communication range d_{max} is increased. Results reveal that, since the target distribution is the same, subchannel allocation has negligible effect on the radar performance. As d_{max} increases, the data rate decreases, due to the decrease in communication SNR. We also see that GBA performs almost optimally and provides a significant improvement with respect to EBA. Optimal solution and proposed GBA allocates more subchannels to radar with long communication range, so that they can use higher SF.

Figure 6 shows the radar and communication performance as a function of PRI (T). If PRI is very low, the combined cost is very high. The reason is that the SF is limited due to the duty cycle constraint. This increases the timing and Doppler errors. There is an abrupt decrease in the cost with increasing PRI. For $T = 1000$ cost increases again. This increase is due to decreasing rate (i.e. $\frac{2^{SF}F_n}{T}$). SF is limited by 12, therefore timing performance keeps fixed. Doppler performance monotonically improves with T . GBA is almost optimal and provides significant performance gain due to clever allocation of subchannels and increasing the spreading factor. There is a tradeoff between radar and communication

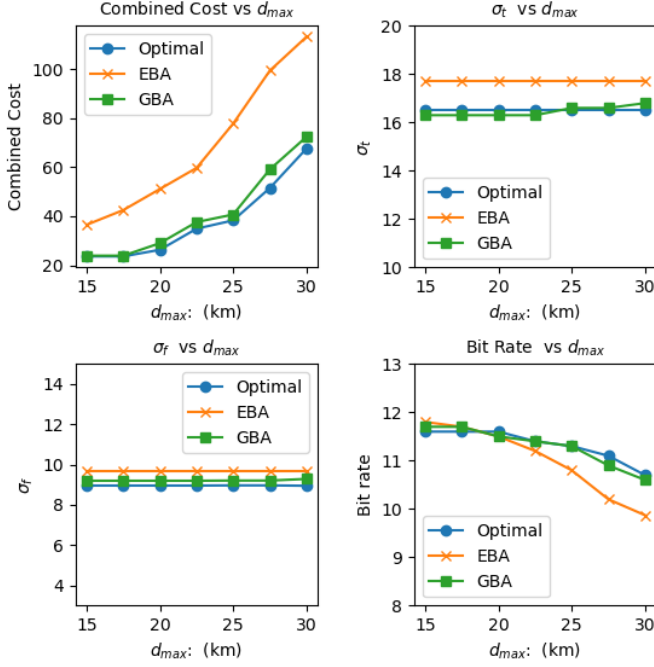


Fig. 5: Performance vs maximum communication range (d_{max})

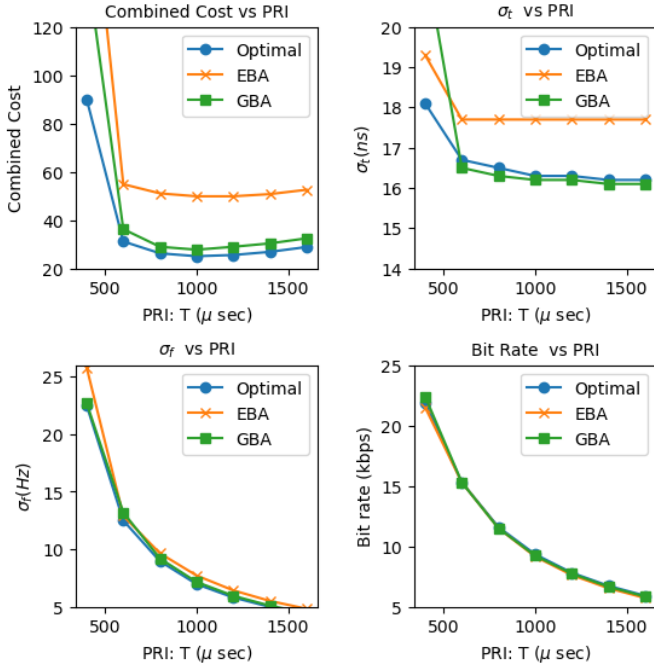


Fig. 6: Performance vs Pulse Repetition Interval (T)

performances, by increasing the PRI.

Figure 7 shows the radar and communication performance as a function of subchannel bandwidth (B). When subchannel bandwidth is lower, chip duration is higher. In that case, available chips (hence maximum possible SF) are smaller. Therefore, as B increases, the data rate increases. As can be seen from Eq. (8) bandwidth does not significantly affect the Doppler performance (bandwidth W_n is cancelled by the

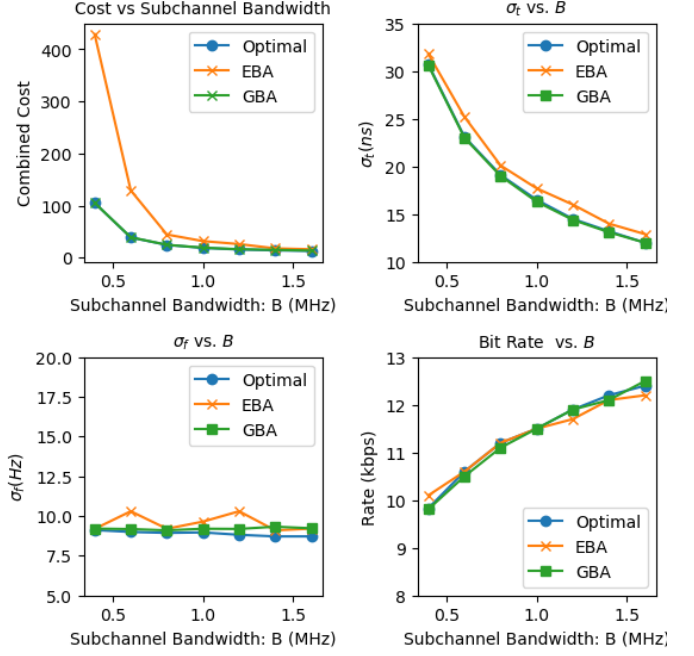


Fig. 7: Performance vs Subchannel Bandwidth (B)

bandwidth in the denominator of the SNR). There are some ripples in the EBA performance. For the EBA method, for $B = [0.4, 0.6, 0.8, 1.0, 1.2, 1.4, 1.6]$ MHz, maximum feasible SF becomes $[6, 7, 7, 7, 8, 8, 8]$, respectively. This affects the choice of spreading factor and is the reason for the zig-zags in the EBA Doppler performance and data rate.

In agreement with Eq. (6) time delay accuracy is inversely proportional to the channel bandwidth, hence the delay error monotonically decreases with bandwidth. GBA method performs almost optimally, and provides significantly better performance than EBA, especially for low bandwidth. As B increases EBA and GBA performances converge. The reason for this is that the timing error ϵ falls below the target and data rate converges to a value due to the limit $SF \leq 12$.

V. CONCLUSIONS

In this paper, we addressed resource allocation problem in a network of radar transceivers that perform joint radar and communication functions. We considered the problem of bandwidth and spreading factor allocation and formulated it as an integer programming problem. We also proposed a greedy bandwidth allocation algorithm along with a benchmark equal bandwidth allocation method. Simulation results reveal that wise allocation of bandwidth is indeed important of joint optimization of radar and communication performances.

There exists a broad area of future work. Firstly, in this work we assumed that there is a command and control center, which poses a single-point-of-failure problem in a military application. Instead of a central unit for data collection, a distributed network of radars can be considered in the future. Decentralized organization of radar transmitters and multihop routing of sensing data can be addressed. Secondly, instead of each radar tracking a separate target, multiple radars jointly

tracking a single target and data fusion at the center can be addressed. In this scenario, data transmission rate for each radar determines the amount of information and the estimation/detection performance at the Command and Control Center.

REFERENCES

- [1] D. Michalski and P. Bernat, "Internet of things in air and missile defence a system solution concept," in *2019 International Conference on Military Technologies (ICMT)*, 2019, pp. 1–5.
- [2] X. Jiang, W. Wu, T. Liu, and L. Hao, "Research on the intelligent air-defense command and decision system based on multi-agent," in *2022 2nd Asia-Pacific Conference on Communications Technology and Computer Science (ACCTCS)*, 2022, pp. 132–136.
- [3] K.-H. Bethke, B. Rode, M. Schneider, and A. Schroth, "A novel noncooperative near-range radar network for traffic guidance and control on airport surfaces," *IEEE Transactions on Control Systems Technology*, vol. 1, no. 3, pp. 168–178, 1993.
- [4] Y. Shen, W. Dai, and M. Z. Win, "Robust power allocation for active and passive localization," in *2013 IEEE International Conference on Communications (ICC)*. IEEE, 2013, pp. 4802–4807.
- [5] A. Panoui, S. Lambotharan, and J. A. Chambers, "Game theoretic power allocation technique for a mimo radar network," in *2014 6th International Symposium on Communications, Control and Signal Processing (ISCCSP)*. IEEE, 2014, pp. 509–512.
- [6] A. Deligiannis, A. Panoui, S. Lambotharan, and J. A. Chambers, "Game-theoretic power allocation and the nash equilibrium analysis for a multistatic mimo radar network," *IEEE Transactions on Signal Processing*, vol. 65, no. 24, pp. 6397–6408, 2017.
- [7] X. Liu, Z.-H. Xu, L. Wang, W. Dong, and S. Xiao, "Cognitive dwell time allocation for distributed radar sensor networks tracking via cone programming," *IEEE Sensors Journal*, vol. 20, no. 10, pp. 5092–5101, 2020.
- [8] T. Tian, T. Zhang, X. Li, N. Li, L. Kong, and M. Ge, "A combinatorial double auction based tasks scheduling approach for multifunction radar network," in *2018 IEEE Radar Conference (RadarConf18)*. IEEE, 2018, pp. 0502–0506.
- [9] M. Xie, W. Yi, T. Kirubarajan, and L. Kong, "Joint node selection and power allocation strategy for multitarget tracking in decentralized radar networks," *IEEE Transactions on Signal Processing*, vol. 66, no. 3, pp. 729–743, 2017.
- [10] D. Wang, Q. Zhang, L. Zhu, Q. Meng, J. Liang, and Y. Luo, "Joint node selection and power allocation optimization for multi-target isar imaging in radar network," in *2022 IEEE International Conference on Signal Processing, Communications and Computing (ICSPCC)*. IEEE, 2022, pp. 1–6.
- [11] C. Shi, L. Ding, W. Qiu, F. Wang, and J. Zhou, "Joint optimization of target assignment and resource allocation for multi-target tracking in phased array radar network," in *2020 IEEE Radar Conference (RadarConf20)*. IEEE, 2020, pp. 1–5.
- [12] W. Yi, Y. Yuan, R. Hoseinnezhad, and L. Kong, "Resource scheduling for distributed multi-target tracking in netted colocated mimo radar systems," *IEEE Transactions on Signal Processing*, vol. 68, pp. 1602–1617, 2020.
- [13] Y. Su, T. Cheng, and Z. He, "Joint resource and detection threshold optimization for maneuvering targets tracking in colocated mimo radar network," *IEEE Transactions on Aerospace and Electronic Systems*, 2023.
- [14] X. Lu, Z. Xu, H. Ren, and W. Yi, "Lpi-based resource allocation strategy for target tracking in the moving airborne radar network," in *2022 IEEE Radar Conference (RadarConf22)*. IEEE, 2022, pp. 1–6.
- [15] J. Dong, C. Shi, J. Zhou, and J. Yan, "Joint radar selection and resource allocation for multi-target tracking in radar network under communication interference," in *2021 International Conference on Control, Automation and Information Sciences (ICCAIS)*. IEEE, 2021, pp. 73–77.
- [16] W. Zhang, C. Shi, J. Zhou, and R. Lv, "Joint aperture and transmit resource allocation strategy for multi-target localization in phased array radar network," *IEEE Transactions on Aerospace and Electronic Systems*, 2022.
- [17] B. K. Chalise, A. F. Martone, and B. H. Kirk, "Harmonic mean sinr maximization-based bandwidth and carrier frequency allocation for distributed radar networks," in *2023 IEEE Radar Conference (RadarConf23)*. IEEE, 2023, pp. 01–06.
- [18] NATO, "Tactical Data Exchange - Link 16 STANAG 5516 Ed 4," 2008. [Online]. Available: [https://nso.nato.int
- [19] —, "Tactical Data Exchange - Link 16 STANAG (RD) 5518 Ed 2," 2015. [Online]. Available: https://nso.nato.int
- [20] F. Liu, C. Masouros, A. P. Petropulu, H. Griffiths, and L. Hanzo, "Joint radar and communication design: Applications, state-of-the-art, and the road ahead," *IEEE Transactions on Communications*, vol. 68, no. 6, pp. 3834–3862, 2020.
- [21] L. Giroto de Oliveira, B. Nuss, M. B. Alabd, A. Diewald, M. Pauli, and T. Zwick, "Joint radar-communication systems: Modulation schemes and system design," *IEEE Transactions on Microwave Theory and Techniques*, vol. 70, no. 3, pp. 1521–1551, 2022.
- [22] F. Liu, Y. Cui, C. Masouros, J. Xu, T. X. Han, Y. C. Eldar, and S. Buzzi, "Integrated Sensing and Communications: Toward Dual-Functional Wireless Networks for 6G and Beyond," *IEEE Journal on Selected Areas in Communications*, vol. 40, no. 6, pp. 1728–1767, 2022.
- [23] M. B. Alabd, L. G. de Oliveira, B. Nuss, W. Wiesbeck, and T. Zwick, "Time-Frequency Shift Modulation for Chirp Sequence based Radar Communications," in *2020 IEEE MTT-S International Conference on Microwaves for Intelligent Mobility (ICMIM)*, 2020, pp. 1–4.
- [24] M. Noor-A-Rahim, M. O. Khyam, A. Mahmud, X. Li, D. Pesch, and H. V. Poor, "Hybrid Chirp Signal Design for Improved Long-Range (LoRa) Communications," *Signals*, vol. 3, no. 1, pp. 1–10, 2022. [Online]. Available: https://www.mdpi.com/2624-6120/3/1/1
- [25] P. Rodriguez-Garcia, G. Ledford, C. Baylis, and R. J. Marks, "Real-time synthesis approach for simultaneous radar and spatially secure communications from a common phased array," in *2019 IEEE Radio and Wireless Symposium (RWS)*, 2019, pp. 1–4.
- [26] S. Şahin and T. Girici, "A novel radar receiver for joint radar and communication systems," in *2023 International Conference on Radar, Antenna, Microwave, Electronics, and Telecommunications (ICRAMET)*. IEEE, 2023, pp. 61–66.
- [27] B. K. Chalise, A. F. Martone, and B. H. Kirk, "Model-and deep learning-based bandwidth and carrier frequency allocation in distributed radar networks," *IEEE Transactions on Aerospace and Electronic Systems*, 2023.
- [28] N. C. Luong, X. Lu, D. T. Hoang, D. Niyato, and D. I. Kim, "Radio resource management in joint radar and communication: A comprehensive survey," *IEEE Communications Surveys & Tutorials*, vol. 23, no. 2, pp. 780–814, 2021.
- [29] V. Petrov, G. Fodor, J. Kokkonen, D. Moltchanov, J. Lehtomaki, S. Andreev, Y. Koucheryavy, M. Juntti, and M. Valkama, "On unified vehicular communications and radar sensing in millimeter-wave and low terahertz bands," *IEEE wireless communications*, vol. 26, no. 3, pp. 146–153, 2019.
- [30] S. Jha, N. M. Balasubramanya, B. K. Chalise, and M. G. Amin, "Performance analysis of lora waveform for joint communications and radar system," *IEEE Transactions on Radar Systems*, vol. 1, pp. 243–248, 2023.
- [31] I. C. Wong, O. Oteri, and W. McCoy, "Optimal resource allocation in uplink sc-fdma systems," *IEEE Transactions on Wireless communications*, vol. 8, no. 5, pp. 2161–2165, 2009.
- [32] A. Hassanien, M. G. Amin, Y. D. Zhang, and F. Ahmad, "Dual-function radar-communications: Information embedding using sidelobe control and waveform diversity," *IEEE Transactions on Signal Processing*, vol. 64, no. 8, pp. 2168–2181, 2015.
- [33] A. R. Al-Salehi, I. M. Qureshi, A. N. Malik, Z. U. Khan, and W. Khan, "Jammer avoidance for dual-function radar-communications using fsk and independent null steering," *Digital Signal Processing*, vol. 114, p. 103057, 2021. [Online]. Available: https://www.sciencedirect.com/science/article/pii/S1051200421000968
- [34] M. A. Richards *et al.*, *Fundamentals of radar signal processing*. McGraw-hill New York, 2005, vol. 1.
- [35] T. J. Abatzoglou and G. O. Gheen, "Range, radial velocity, and acceleration mle using radar lfm pulse train," *IEEE Transactions on Aerospace and Electronic Systems*, vol. 34, no. 4, pp. 1070–1083, 1998.
- [36] A. Dogandzic and A. Nehorai, "Cramer-rao bounds for estimating range, velocity, and direction with an active array," *IEEE transactions on Signal Processing*, vol. 49, no. 6, pp. 1122–1137, 2001.
- [37] J. A. Johnson and M. L. Fowler, "Cramer-rao lower bound on doppler frequency of coherent pulse trains," in *2008 IEEE International Conference on Acoustics, Speech and Signal Processing*. IEEE, 2008, pp. 2557–2560.
- [38] T. S. Rappaport, *Wireless Communications: Principles and Practice*. Cambridge University Press, 2024.

- [39] T. Elshabrawy and J. Robert, "Closed-form approximation of LoRa modulation BER performance," *IEEE Communications Letters*, vol. 22, no. 9, pp. 1778–1781, 2018.